Parthasarathy and Vivekanandan *Health Inf Sci Syst (2018) 6:5*
https://doi.org/10.1007/s13755-018-0043-3

Health Information Science and Systems

RESEARCH

Investigation on uric acid biosensor model for enzyme layer thickness for the application of arthritis disease diagnosis

P. Parthasarathy* and S. Vivekanandan

Abstract

Uric acid biosensors for arthritis disease has been developed for the specific selection of uricase enzyme film thickness coated over the TiO_2–CeO_2 nano-composite matrix is modelled mathematically. This model is purely based on R-diffusion conditions with irreversible first-order catalytic reactions. By arithmetical method, the impact of the thickness of enzyme layer on the current response of the biosensor was explored. This article displays a structure for choice of the enzyme layer thickness, guaranteeing the adequately stable sensitivity of a biosensor in a required extent of the maximal enzymatic rate. The numerical outcomes showed subjective and sensible quantitative information for oxidation current due to uric acid also shows the maximum change in the biosensor current response due to the change in membrane thickness, which will be more suitable for uric acid biosensor for the application of arthritis disease diagnosis.

Keywords: First-order catalytic reactions, Uric acid sensor, Enzyme layer thickness, Modelling

Introduction

Biosensors are logical device that depend on the immediate coupling of an immobilized naturally powerful compound with an electronic amplifier and transducer, which converts the biochemical signal to an electronic signal [1, 2]. The biosensor signal is relative to the concentration of analyte measured or a group of analytes. The biosensors are characterized by the sort of transducer utilized. Amperometric biosensors measure the current on the electrode because of direct oxidation of the results of the biochemical response. In the event of the amperometric biosensors, the potential at the electrode is kept consistent where the present current is measured.

The amperometric biosensors are dependable, clinical moderately, shabby and very delicate for clinical conditions, mechanical and industrial purposes. From the publication of Clark and Lyons [3], the amperometric biosensors ended up plainly one of the common and perspective examples of organic chemistry. The comprehension of the dynamic and kinetic regularities of biosensors is of critical noteworthy for their outline. Mathematical and scientific models can illuminate such regularities. The general highlights of amperometric reaction were investigated in the distributions of Mell and Maloy [4]. Some later reports were likewise dedicated to the demonstrating and examination of the amperometric biosensor reaction [5, 6].

Enzymes immobilized in the biosensors are used to distinguish the grouping of a particular analyte because of the natural acknowledgment between the analyte and the immobilized enzyme [7].

Thick enzyme layers have been created by means of cross linking [8], entrapment [9] and, by physical deposition [10]. The reason for these methodologies is to immobilize the enzymes in their dynamic region. As of late, we detailed that enzymes such as uricase, glucose oxidase, glutamate oxidase and galactosidase can be coated using various techniques to yield thick, active enzyme layers which were used for the improvement of highly sensitive biosensors [11]. Numerical models, solutions and arrangements of enzymes prepared by different procedures, for example, immobilization in scattered carbon nanotubes, electro polymerization and encapsulation in

*Correspondence: arjunsarathii@gmail.com
School of Electrical Engineering, VIT University, Vellore, Tamilnadu, India

membranes have been accounted [12, 13]. In this note, the unfaltering state amperometric current of uricase layers kept is modelled as a function of the enzyme layer thickness. This article mainly provides the structure for choice of the enzyme film thickness, ensuring the satisfactorily stable biosensor reaction in a required scope of the enzymatic response rate has been portrayed.

Mathematical model formulation

A diagrammatic portrayal of the TiO_2–CeO_2 thin film electrode over a uniform uricase enzyme layer is coated is delineated in Fig. 1.

The amperometric response of uric acid is because of the enzymatic change in uric acid to hydrogen peroxide and allontoin as a by-product:

$$\text{Uric acid} + H_2O + O_2 \longrightarrow \text{UricaseAllantoin} + CO_2 + H_2O_2$$

$$H_2O_2 \rightarrow O_2 + 2H^+ + 2e^-$$

The above reaction demonstrates that for each and every molecule of uric acid reacts, one molecule of hydrogen peroxide is formed and again it undergoes oxidation at the electrode surface to form a free electron.

As the movement of uric acid inside the enzyme film happens by dissemination, we predicate that the amount of concentration $\boldsymbol{u_1}$ of uric acid inside the film is administrated by the one-dimensional reaction–diffusion equation:

$$K_1^e \frac{d^2u_1}{dx^2} - Du_1 = 0 \text{ for } 0 \le x \le \alpha \tag{1}$$

where K_1^e is the powerful dispersion coefficient of uric acid ($m^2\ s^{-1}$), D is the forward reaction response rate steady (s^{-1}) of the reaction between uric acid and oxygen, x is the typical separation to the terminal electrode and α is the thickness (in micron) of the enzyme film appeared in Fig. 2.

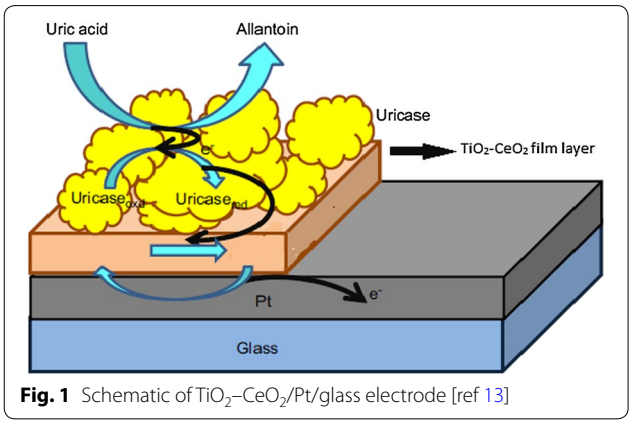

Fig. 1 Schematic of TiO_2–CeO_2/Pt/glass electrode [ref 13]

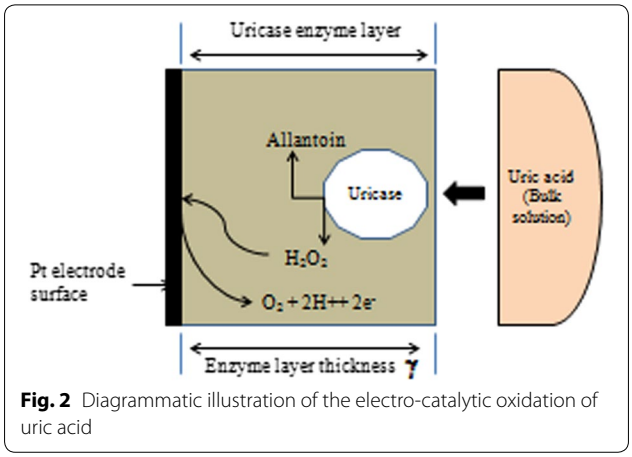

Fig. 2 Diagrammatic illustration of the electro-catalytic oxidation of uric acid

In Eq. (1), we assume that the reaction rate of uric acid is first order in the uric acid concentration (Du_1). In perspective view of the test confirmation of Fig. 5 [14], this is a substantial presumption for the uric acid concentrations utilized as a section in this work. Equation (1) additionally accepts that the response is irreversible or that the retrogressive response (backward reaction) continues at a substantially littler rate and that the oxygen fixation is adequately high as tentatively watched for the enzyme electrode [7].

Equation (1) is liable to the accompanying limit (boundary) conditions:

$$\frac{du}{d_x} = 0 \text{ at } x = 0 \tag{2}$$

$$-K_1^e \frac{du_1}{d_x} = g_1\left(u_1 - u_1^{\infty}\right) \text{ at } x = \alpha \tag{3}$$

where u_1^{∞} is the uric acid concentration in the mass.

The principal (1st boundary condition) limit condition expresses that uric acid itself isn't electrochemically dynamic and subsequently does not oxidize or lessen on the surface of the electrode ($x = 0$). This is to be sure the case at the applied potential of + 0.6 V versus AgCl/Ag.

The second limit condition expresses that, at the enzyme film-electrolyte interface, the mass transport by dispersion in the film parallels the convective transport in the electrolyte, with g_1 the convection coefficient of uric corrosive ($m\ s^{-1}$).

The enzymatically created H_2O_2 is electrochemically oxidized on the surface of the pt electrode:

$$H_2O_2 \rightarrow O_2 + 2H^+ + 2e^-$$

Subsequently, the focus p_2 of H_2O_2 inside the uricase enzyme film is represented by the accompanying one-dimensional reaction dispersion condition:

$$K_2^e \frac{d^2 p_2}{dx^2} + Du_1 = 0 \text{ for } 0 \le x \le \alpha \tag{4}$$

with K_2^e is the compelling dissemination (diffusion) coefficient of H_2O_2, the above equation is liable to the accompanying limit (boundary) conditions:

$$p_2 = 0 \text{ at } x = 0 \tag{5}$$

$$-K_2^e \frac{dp_2}{d_x} = g_2\left(p_2 - p_2^\infty\right) \text{ at } x = \alpha \tag{6}$$

where p_2^∞ is the amount concentration of H_2O_2 in the mass (in this work we assumed 0 mol m^{-3}).

The principal limit condition (1st condition) expresses that at the applied potential (+ 0.6 V vs. Ag/AgCl), hydrogen peroxide is mass transport restricted inside the enzyme film and its concentration ends up noticeably zero on the surface of the terminal electrode. The second limit (boundary) condition is indistinguishable to Eq. (3). An Eq. (1) through (6) is solved analytically for p_2 beneath.

Equation derivation

Equation (1) is a second order differential equation with consistent coefficients for which the general solution arrangement is given by:

$$u_1 = Pcosh\sqrt{D/K_1^e}x + R\sinh\sqrt{D/K_1^e}x \tag{7}$$

with P and R two integration constants, whose esteem can be resolved from the limit conditions (2) and (3). Condition (2) yields R = 0 while Eq. (3) yields:

$$P = \frac{u_1^\infty}{cosh\sqrt{D/K_1^e}\gamma + \sqrt{\frac{D/K_1^e}{g_1}}\sinh\sqrt{D/K_1^e}\alpha} \tag{8}$$

yielding the accompanying answer for $u1$:

$$u_1 = u_1^\infty \frac{cosh\sqrt{D/K_1^e}x}{cosh\sqrt{D/K_1^e}\alpha + \sqrt{\frac{D/K_1^e}{g_1}}\sinh\sqrt{D/K_1^e}\alpha} \tag{9}$$

With the solution of $u1$, the general arrangement of Eq. (4) can be found:

$$p_2 = -P\frac{K_1^e}{K_2^e}cosh\sqrt{D/K_1^e}x + Sx + T \tag{10}$$

Table 1 Diffusion coefficients of uric acid and H_2O_2 in water at 25 °C

Solute	Ki m^2 s^{-1}	Reference
Uric acid	6.7×10^{-10}	[15]
Hydrogen peroxide	1.3×10^{-9}	[15]

The two integration constants S and T which can be found from the limit (boundary) conditions (5) and (6) result in the accompanying answer for $p2$:

$$p_2 = \frac{K_1^e}{K_2^e}P\left(1 - cosh\sqrt{D/K_1^e}x\right) + \frac{K_1^e P}{K_2^e + g_2\alpha}\left[\sqrt{\frac{D}{K_1^e}}\sinh\sqrt{\frac{D}{K_1^e}}\alpha + \frac{g_2}{K_2^e}\left(cosh\sqrt{D/K_1^e}\alpha - 1\right)\right]x \tag{11}$$

The current density I (Am^{-2}) because of the oxidation of hydrogen peroxide is relative to the focus slope (concentration) of hydrogen peroxide on the electrode surface as per:

$$I = -nFK_2^e\frac{dp_2}{dx} \text{ at } x = 0 \tag{12}$$

where n is the quantity (number) of the electrons traded in the oxidation of one molecule of H_2O_2 and F is Faraday's constant. By utilizing Eqs. (7–11), I can be derived by differentiation according to Eq. (12).

This results in the accompanying closed-form expression for the current density:

$$I = \frac{-nFK_1^e Du_1^\infty}{K_2^e + g_2\alpha} \times \frac{K_2^e\sqrt{\frac{D}{K_1^e}}\sinh\sqrt{\frac{D}{K_1^e}}\gamma + g_2\left(cosh\sqrt{\frac{D}{K_1^e}}\alpha - 1\right)}{cosh\sqrt{\frac{D}{K_1^e}}\alpha + \frac{\sqrt{D/K_1^e}}{g_1}\sinh\sqrt{D/K_1^e}\alpha} \tag{13}$$

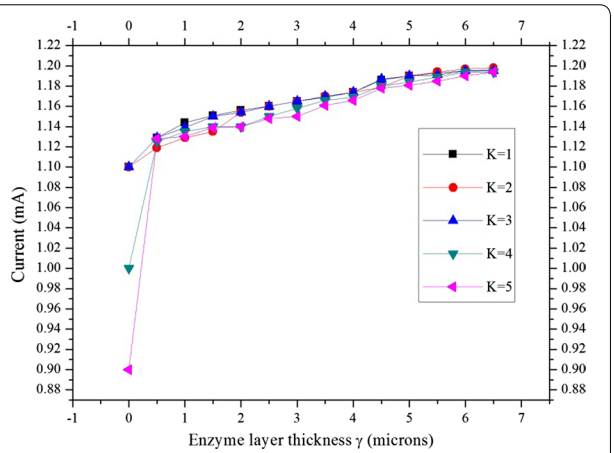

Fig. 3 Simulated currents as a function of the enzyme layer thickness for different reaction rate constant of D (represented as k in all the figures below) values measures up to 1, 2, 3, 4 and 5 s^{-1} from base to top

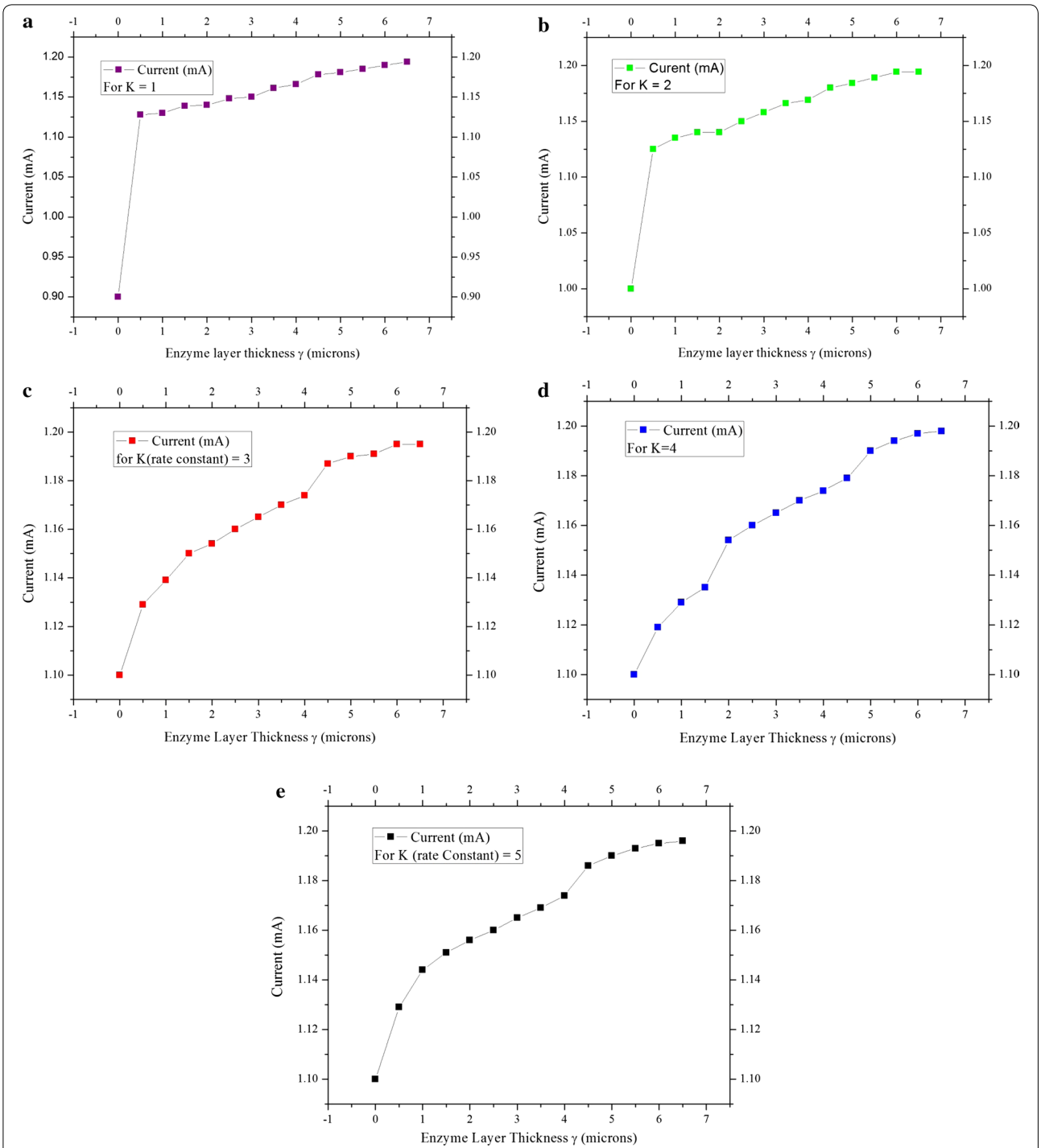

Fig. 4 **a** Enzyme layer thickness (microns) versus current (mA) for D = 1 s^{-1}. **b** Enzyme layer thickness (microns) versus current (mA) for D = 2 s^{-1}. **c** Enzyme layer thickness (microns) versus current (mA) for D = 3 s^{-1}. **d** Enzyme layer thickness (microns) versus current (mA) for D = 4 s^{-1}. **e** Enzyme layer thickness (microns) versus current (mA) for D = 5 s^{-1}

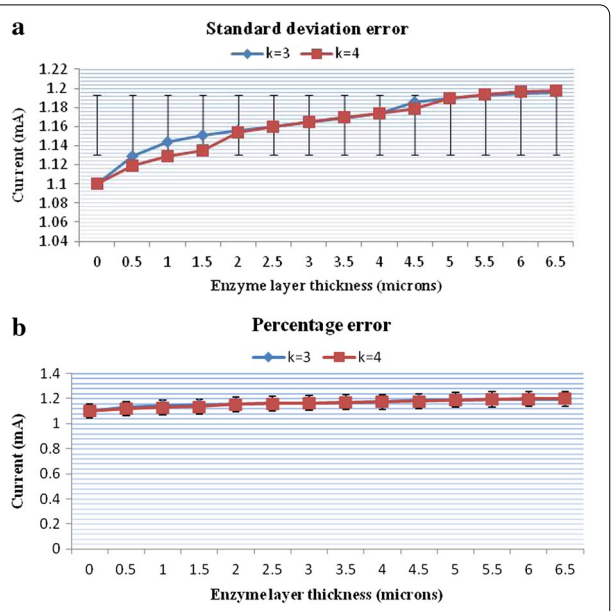

Fig. 5 **a** Standard deviation error graph different D (D = 3 and 4) values. **b** Percentage error graph different D (D = 3 and 4) values

Results and discussion

The amperometric response of the uricase enzyme film was ascertained utilizing Eq. (13) in view of esteems for the diffusion coefficients found in literature and recorded in Table 1.

As per the Ref. [15] on the diffusion of organic solutes in bio-films (which we acknowledge to resemble like the enzyme films of this work), we expected that the proportion of the effective diffusion coefficient inside the enzyme film to the diffusion coefficient in water equals 0.25. The convection coefficients for uric acid and hydrogen peroxide were assessed assuming:

$$g_i = \frac{K_i}{t} \tag{14}$$

where t represents the diffusion layer thickness (which is assumed to be 100 μm)

The amperometric response of the uricase enzyme on a TiO_2–CeO_2 film to a uric acid concentration of 5 mM is plotted in Fig. 3 as a function of the thickness of the uricase enzyme layer for various values of the reaction rate constant D (D = 1, 2, 3, 4 and 5).

As can be found in the accompanying figures, the current because of uric acid unequivocally increments as the thickness of the enzyme layer increase. Figure 4a–e additionally shows that when the film achieves a specific thickness (esteem contingent upon the rate constant); the current levels off and achieves a most extreme.

This kind of behaviour can be comprehended as follows:

At the point when the film thickness is small, almost no uric acid is converted into hydrogen peroxide and so the current is less. As the film thickness increases, more concentration of uric acid reacts with uricase enzyme to form hydrogen peroxide which again reduces at the redox centre in the electrode surface to give more number of free electrons which increases the current value. For a specific thickness, all of the uric acid that enters the film is converted to hydrogen peroxide and the current stretches to maximum. At the point when the film winds up noticeably thicker, the current drops as part of the hydrogen peroxide that is formed in the film diffuses out before it reacts at the electrode.

It was found that the current reaches maximum value of 1.9 mA when the thickness of the enzyme layers is around 65 microns with the reaction rate constant of 5 s^{-1}. It is also noted that there is only a minimal changes in the current value for different D values (inferred from the Fig. 3) and also standard deviation and percentage errors was calculated for values of D (for D = 3 and D = 4) accordingly (Fig. 5).

Conclusions

The amperometric current response of uricase enzyme layers coated by physical adsorption method over TiO2–CeO_2 thin film matrix was modelled as a function of the thickness of the enzyme layer. The model is based on reaction–diffusion equations with irreversible first-order reactions. The mathematical model based on this reaction–diffusion equation is successfully used to investigate the enzyme layer thickness. The outcome shows that the current reaches maximum value of 1.9 mA when the thickness of the enzyme layers is around 65 microns with the reaction rate constant of 5 s^{-1}. It is likewise noticed that there is only a minimal changes in the current value for different D values. The sensitivity of biosensors can be increased by selecting the appropriate enzyme layer thickness enzymatic reaction rate.

Publisher's Note

Received: 23 February 2018 Accepted: 6 April 2018
Published online: 23 April 2018

References

1. Scheller F, Schubert F. Biosensors, vol. 7. Amsterdam: Elsevier; 1992.
2. Chaubey A, Malhotra BD. Mediated biosensors. Biosens Biolectron. 2002;17:441–56.

3. Mell CD, Maloy JT. A model for the amperometric enzyme electrode obtained through digital simulation and applied to the glucose oxidase system. Anal Chem. 1975;47:299–307.
4. Mell CD, Maloy JT. Amperometric response enhancement of the immobilized glucose oxidase enzyme electrode. Anal Chem. 1976;48:1597.
5. Sorochinskii VV, Kurganov BI. Steady-state kinetics of cyclic conversions of substrate in amperometric bienzyme sensors. Biosens Bioelectron. 1996;11(3):225–38.
6. Yokoyama K, Kayanuma Y. Cyclic voltammetric simulation for electrochemically mediated enzyme reaction and determination of enzyme kinetic constants. Anal Chem. 1998;70(16):3368–76.
7. Davis G. Electrochemical techniques for the development of amperometric biosensors. Biosensors. 1985;1(2):161–78.
8. Kennedy JF, Kalogerakis B, Cabral JMS. Surface immobilization and entrapping of enzymes on glutaraldehyde crosslinked gelatin particles. Enzyme Microbial Technol. 1984;6(3):127–31. https://doi.org/10.1016/0141-0229(84)90119-4.
9. Chen X, Hu Y, Wilson GS. Glucose microbiosensor based on alumina sol-gel matrix/electropolymerized composite membrane. Biosens Bioelectron. 2002;17(11–12):1005–13. https://doi.org/10.1016/S0956-5663(02)00093-3.
10. Chen X, Matsumoto N, Hu H, Wilson GS. Electrochemically mediated electrodeposition/electropolymerization to yield a glucose microbiosensor with im-proved characteristics. Anal Chem. 2002;74(2):368–72. https://doi.org/10.1021/ac015628m.
11. Lyons MEG. Transport and kinetics at carbon nanotube-redox enzyme composite modified electrodes biosensors. Int J Electrochem Sci. 2009;4(1):77–103.
12. Bartlett PN, Whitaker RG. Electrochemical immobilization of enzymes: Part I. Theory. J Electroanal Chem Interfacial Electrochem. 1987;224(1–2):27–35. https://doi.org/10.1016/0022-0728(87)85081-7.
13. Parthasarathy P, Vivekanandan V. A numerical modelling of an amperometric-enzymatic based uric acid biosensor for GOUT arthritis diseases. Inform Med Unlocked. 2018. https://doi.org/10.1016/j.imu.2018.03.001.
14. Stewart PS. Diffusion in biofilms. J Bacteriol. 2003;185(5):1485–91. https://doi.org/10.1128/JB.185.5.1485-1491.2003.
15. Longsworth LG. Diffusion in liquids and the Stokes–Einstein relation. In: Shedlovsky T, editor. Electrochemistry in biology and medicine. New York: Wiley; 1955. p. 225–47.